

## Development of method for in-service crack detection based on distributed fiber optic sensors

Branko Glisic and Daniele Inaudi

*Structural Health Monitoring* published online 9 August 2011

DOI: 10.1177/1475921711414233

The online version of this article can be found at:

<http://shm.sagepub.com/content/early/2011/08/06/1475921711414233>

A more recent version of this article was published on - Feb 28, 2012

---

Published by:



<http://www.sagepublications.com>

Additional services and information for *Structural Health Monitoring* can be found at:

**Email Alerts:** <http://shm.sagepub.com/cgi/alerts>

**Subscriptions:** <http://shm.sagepub.com/subscriptions>

**Reprints:** <http://www.sagepub.com/journalsReprints.nav>

**Permissions:** <http://www.sagepub.com/journalsPermissions.nav>

[Version of Record - Feb 28, 2012](#)

[>> OnlineFirst Version of Record - Aug 9, 2011](#)

[What is This?](#)

# Development of method for in-service crack detection based on distributed fiber optic sensors

Branko Glisic<sup>1</sup> and Daniele Inaudi<sup>2</sup>

## Abstract

Many bridges worldwide are approaching the end of their lifespan and it is necessary to assess their health condition in order to mitigate risks, prevent disasters, and plan maintenance activities in an optimized manner. Fracture critical bridges are of particular interest since they have only little or no load path redundancy. Structural health monitoring (SHM) has recently emerged as a branch of engineering, which aim is to improve the assessment of structural condition. Distributed optical fiber sensing technology has opened new possibilities in SHM. A distributed deformation sensor (sensing cable) is sensitive at each point of its length to strain changes and cracks. Such a sensor practically monitors a one-dimensional strain field and can be installed over all the length of the monitored structural members, thereby providing with integrity monitoring, i.e. direct detection and characterization (including recognition, localization, and quantification or rating) of local strain changes generated by damage. Integrity monitoring principles are developed and presented in this article. A large scale laboratory test and a real on-site application are briefly presented.

## Keywords

fiber-optic sensors, fracture critical bridges, in-service crack detection, structural health monitoring, Brillouin scattering

## Introduction

Fracture critical members are components in tension whose failure is expected to result in the collapse of the bridge or the inability of the bridge to perform its function.<sup>1</sup> Fracture critical bridges are those which contain fracture critical members. Practically, a fracture critical bridge by design has little or no load path redundancy with respect to fracture critical members. Thus, the fracture critical bridge is not structurally deficient unless subjected to damage or deterioration – even a new bridge can be fracture critical (by design). Approximately 11% of US bridges are identified as fracture critical,<sup>2</sup> which corresponds to more than 60,000 bridges. Aging of these bridges and associated damage and deterioration induced by environmental degradation, wear, and episodic events like earthquake or impact, raise concerns about their safety and longevity.

The I35W Minneapolis Bridge was a fracture critical bridge that collapsed due to design error (bowing of the gusset plate due to inadequate dimensioning).<sup>3</sup> It is a sad example which demonstrates the catastrophic consequences of a failure of a bridge:<sup>4</sup> loss of 13 lives, while

145 people were injured; unavailability of the river crossing generated economic losses of US\$ 400,000 per day for road-users. In addition, losses for the Minnesota economy were estimated to US\$ 17 million in 2007 and to US\$ 43 million in 2008. The cost of rebuilding the bridge was approximately US\$ 234 million.<sup>5</sup>

In order to decrease the risk of failure and to help optimize maintenance activities, a modern structure can be made capable to 'generate' and 'communicate' information concerning the changes in its structural health condition and potential damage or deterioration, to responsible operators and decision makers, in-time – automatically or on-demand, and reliably. To achieve this, a modern structure should be equipped with a

<sup>1</sup>Department of Civil and Environmental Engineering, Princeton University, E330 EQuad, Princeton, NJ 08544, USA.

<sup>2</sup>SMARTEC SA, Via Poblette 11, CH-6928 Manno, Switzerland.

## Corresponding author:

Branko Glisic, Princeton University, E330 EQuad, Princeton, NJ 08544, USA  
Email: bglisic@princeton.edu

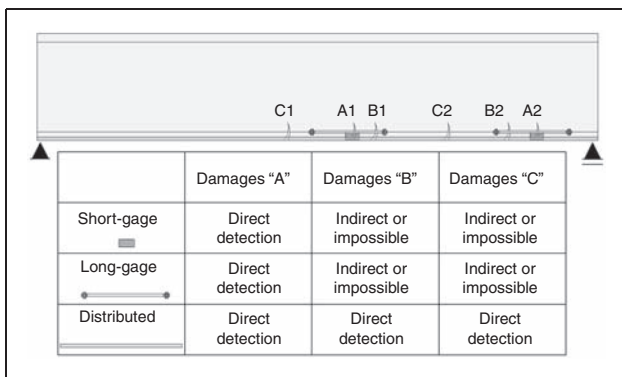


**Figure 1.** Schematic comparison between damage detection capabilities of short-gage, long-gage, and distributed sensors (schematic representation does not refer to a real case).

'nervous system', a 'brain' and 'voice lines', i.e. with a structural health monitoring (SHM) system which is continuously in operation and able to sense parameters reflecting structural condition. Depending on the level of sophistication, the monitoring system should be able to automatically detect damage (level 1), point to the location of the damage (level 2), quantify or rate the severity of the damage (level 3), and estimate of residual lifespan (level 4).<sup>6</sup> The information about the damage should be reported to bridge managers, who can act upon its reception.

Standard monitoring practice is based on the choice of a reduced number of points that are supposed to be representative of the structural behavior, and their instrumentation with discrete sensors, short-gage or long-gage. If short-gage sensors are used, the monitoring will give interesting information on the local behavior of the construction materials, but might miss behaviors and degradations that occur at locations that are not instrumented. Using long-gage sensors, it becomes possible to cover a significant volume of a structure with sensors enabling global monitoring, i.e. any phenomenon that has an impact on the global structural behavior is detected and characterized. However, reliability of detection and characterization of damage that occurs in the locations far from the sensors remains challenging, since it depends on sophisticated algorithms whose performance is often decreased due to various influences that may 'mask' the damage, such as high temperature variations, load changes, outliers, and missing data in monitoring results.<sup>7</sup>

Distributed sensing technology offers solutions for improved and reliable damage detection. The qualitative difference between the monitoring performed using discrete and distributed sensors is the following: discrete sensors monitor strain or average strain in discrete points, while the distributed sensors are capable of one-dimensional (linear) strain field monitoring. Distributed sensors can be installed along the whole length of

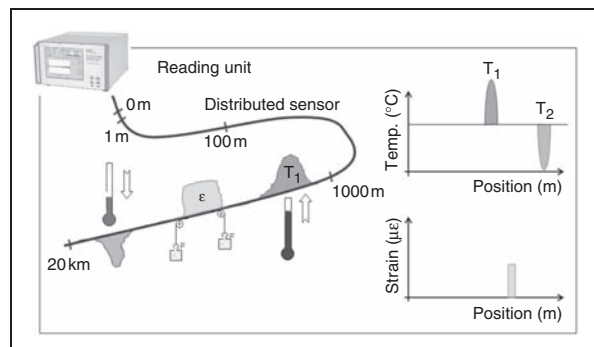


**Figure 2.** Schematic representation of a distributed sensor.

structure and in this manner each cross-section of the structure is practically instrumented. The sensor is sensitive at each point of its length and it provides for direct damage detection, avoiding the use of sophisticated algorithms. In this manner integrity monitoring of structure can be reliably performed. A schematic comparison between damage detection capabilities of sensors with varying gauge-length and spatial arrangement is given in Figure 1.

## Distributed sensing

A distributed sensor (or sensing cable) can be represented by a single cable which is sensitive at any point along its length. Hence, one distributed sensor can replace a large number of discrete sensors. Since the cable is continuous, it provides for monitoring of a one-dimensional strain field, i.e. it provides a distribution of the measured strains along the sensor. Another advantage is that it only requires a single connection cable to transmit the information to the reading unit, instead of a large number of connecting cables required in the case of wired discrete sensors. Finally, distributed sensors are less difficult and more economical to install and operate. A distributed sensor is schematically represented in Figure 2.

Distributed sensing has been made possible through recent developments in the domain of fiber optic sensing technologies. There are three main physical principles used in distributed sensing: Rayleigh scattering (e.g. Ref. 8), Spontaneous Brillouin scattering (e.g. Ref. 9) and Stimulated Brillouin scattering (e.g. Ref. 10). Techniques based on Rayleigh scattering and Spontaneous Brillouin scattering are limited to short length, while the techniques based on Stimulated Brillouin scattering allow for monitoring of very long structures. For this reason, it is presented here in more detail.

The active stimulation of Brillouin scattering is achieved by using two optical light waves. In addition to the optical pulse, usually called the pump, a continuous wave optical signal, the so-called probe signal, is

used to probe the Brillouin frequency profile of the fiber. The interaction leads to a larger scattering efficiency, resulting in an energy transfer from the pulse to the probe signal and an amplification of the probe signal. Brillouin scattering is simultaneously sensitive to both strain and temperature, and in order to discriminate the strain it is necessary to perform temperature compensation. For this purpose a separate distributed temperature sensor is installed in a close proximity of the strain sensor, assuming that both sensors will be subjected to the same temperature variations. The temperature sensor contains the optical fibers that are placed in an internal tube which accommodates extra lengths of the fibers. This makes fibers strain free and practically sensitive only to temperature. The strain is discriminated from the measurement as a linear combination of strain sensor measurement and temperature sensor measurement at each point along the sensors, using calibration coefficients provided by manufacturer. Monitoring systems based on stimulated Brillouin scattering are less sensitive to cumulated optical losses that may be generated in sensing cables due to manufacturing and installation, and allow for monitoring of exceptionally large lengths.<sup>11</sup> For example, in the case of strain monitoring, a single reading unit with two channels can operate measurement over lengths of 10 km, while in the case of temperature monitoring, lengths of 50 km can be reached. Remote modules can be used to triple the monitoring lengths. Typical performance of the system used in monitoring of bridges is given in Table 1.<sup>12</sup>

The typical performance given in Table 1 is defined based on the real application presented later in the text.<sup>12</sup> However, the performance can be modified depending on the project requirements, since the accuracy of measurement, the range of measurands, and the measurement time per channel are interdependent. The strain range can be extended from  $-10,000 \mu\epsilon$  to  $+10,000 \mu\epsilon$ , and temperature range from  $-40^\circ\text{C}$  to  $+85^\circ\text{C}$  ( $-40^\circ\text{F}$  to  $+185^\circ\text{F}$ ), but as a consequence the

measurement time per channel should increase proportionally to the increase of range of measurands, or the accuracy of measurements should decrease proportionally to the range of measurands.

The spatial resolution and the spatial sampling interval are measurement parameters that are explained in the next section. They are usually determined based on the project requirements and set into the monitoring system by the user, through the user interface. Since the stability of the speed of the light in the optical fibers is very high and the stability of the light source (laser) as well, the error of the system in defining spatial resolution and spatial sampling interval is negligible.

When strain sensing is required, the optical fiber must be bonded to the host material over the whole length. The transfer of strain is to be complete, with no losses due to relative motion. Therefore, an excellent bond between strain optical fiber and the host structure is to be guaranteed. To allow such a good bond it has been recommended to integrate the optical fiber within a tape, similarly to how reinforcing fibers are integrated in composite materials. To produce such a tape, a glass fiber reinforced thermoplastic with polyphenylene sulfide (PPS) matrix has been selected.<sup>13</sup> This material has excellent mechanical and chemical resistance properties. Since its production involves heating to high temperatures (in order to melt the matrix of the composite material) it is necessary for the fiber to withstand this temperature without damage. In addition, the bond between the optical fiber coating and the matrix has to be guaranteed. Polyimide-coated optical fibers fit these requirements and were therefore selected for this design. The details of thermoplastic composite tape with integrated optical fiber are given in Figure 3.

## Crack detection with distributed sensor

Although a distributed deformation sensor is sensitive to strain at every point of its length  $L_D$ , it measures at

**Table 1.** Typical performance of the distributed sensing system used for monitoring of bridges

Strain resolution	$3 \mu\epsilon$
Strain accuracy	$\pm 21 \mu\epsilon$
Strain range	$-5000 \mu\epsilon$ to $+10,000 \mu\epsilon$
Crack detection	Opening of 0.5 mm over 100 mm (1/50" over 4")
Temperature accuracy	$\pm 1^\circ\text{C}$ ( $\pm 1.8^\circ\text{F}$ )
Temperature range	$-30^\circ\text{C}$ to $+85^\circ\text{C}$ ( $-22^\circ\text{F}$ to $+185^\circ\text{F}$ )
Spatial resolution	1 m (3'-3")
Sampling interval	0.1 m (4")
Total bridge length equipped with sensors	Several kilometers, depends on application
Measurement time per channel	< 10 min
Measurement time for whole system	< 2 h, depends on the number of channels and the number of reading units

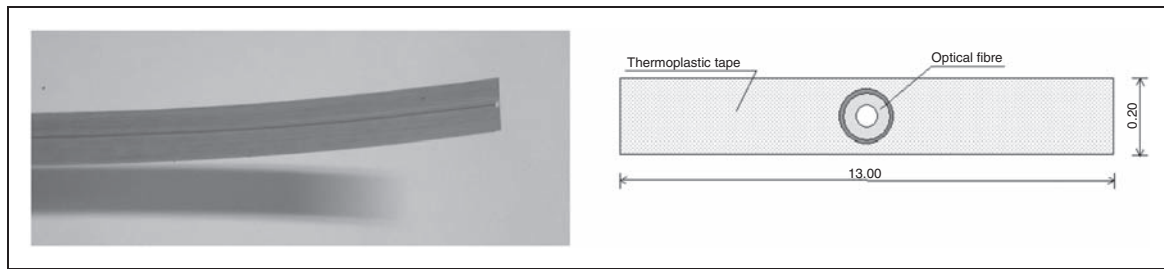


Figure 3. Distributed sensor details, units in millimeters (mm).

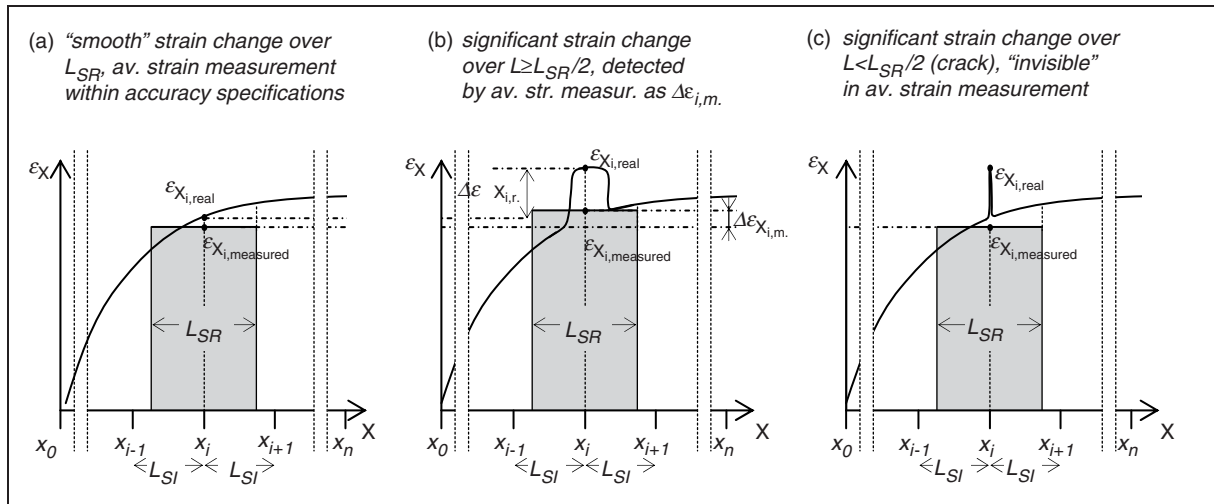


Figure 4. Simplified presentation of the principle of distributed sensor measurement.

discrete points that are spaced by a constant value, called the sampling interval and denoted with  $L_{SI}$ , and the measured parameter is actually an average strain measured over a certain length, called the spatial resolution and denoted with  $L_{SR}$ .<sup>14</sup> Coordinates  $x_i$  of discrete measurement points (defined by the sampling interval) are defined as follows:  $x_i = x_0 + i \cdot L_{SI}$ ,  $i=1,2,3,\dots,n$ , where  $x_0$  is the coordinate of the first point on the sensor and  $n=\text{integer}(L_D/L_{SI}) - 1$ , unless  $x_0$  coincide with the beginning of the first interval  $L_{SI}$ , in which case  $n=\text{integer}(L_D/L_{SI})$ . The spatial resolution can be considered as a gauge length over which the strain is averaged. Thus, the strain measurement values are given in discrete points with coordinates  $x_i$  which are spaced by sampling intervals  $L_{SI}$ . Value at each point  $x_i$  is actually an average strain obtained by integration over the length of spatial resolution  $L_{SR}$ . Both parameters are set by the user depending on project requirements, and in order to include entire length of the sensor in the measurements it is recommended for sampling interval not to be larger than a half of the spatial resolution (see Figure 4). These parameters and the principle of distributed sensor measurement are presented, in a simplified manner, in Figure 4.

Let the real strain distribution along the sensor without crack be as presented in Figure 4(a). For each point with coordinate  $x_i$ , the strain is averaged over the segment  $(x_i-L_{SR}/2, x_i+L_{SR}/2)$  as presented in Figure 4(a) (gray area represents equivalent average strain), and the value of the measurement is attributed to the point  $x_i$ . The difference between real and measured strain at point  $x_i$  is small ( $\epsilon_{X,i,\text{measured}} \approx \epsilon_{X,i,\text{real}}$ ) and depends on the strain change along the length of the spatial resolution.

Significant strain changes that occur over lengths shorter than the spatial resolution (e.g. strain concentrations at locations of geometric imperfections, change in cross-sectional properties, or at locations where a concentrated load is applied), but not shorter than its half, are detected and localized, but not accurately measured, as shown in Figure 4(b) ( $0 < |\Delta\epsilon_{X,i,m}| < < |\Delta\epsilon_{X,i,r}|$ ).

This principle, however, is not valid for abrupt strain changes or concentrated strains in sensing optical fiber such as generated by cracks, see Figure 4(c). In these cases the measurement resulting from a distributed sensing system can possibly lead to important measurement errors. Even very high strain changes that occur over lengths shorter than one-half of the spatial

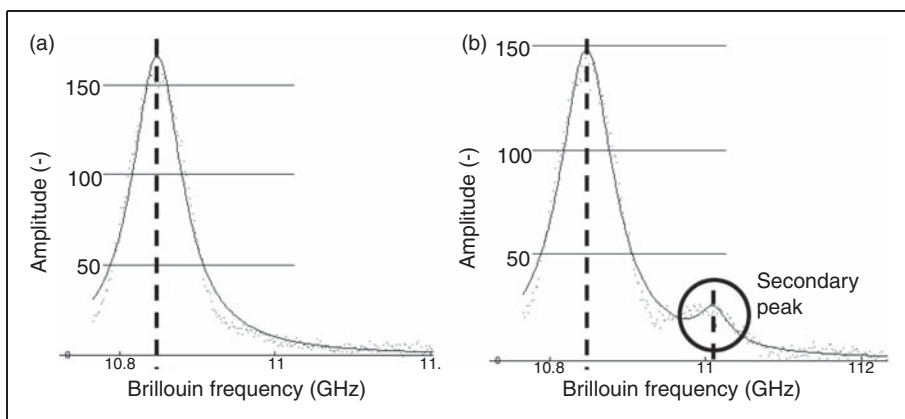


**Figure 5.** Main peak of Brillouin frequency generated by strain change in one point of the sensing optical fiber, and both main and secondary peaks generated in case of crack occurrence (courtesy of Omnisens SA, Switzerland).

resolution are practically ‘invisible’ for the system in common mode of functioning, as shown in Figure 4(c). In addition, high local strains can lead to physical rupture of sensing optical fiber.

In order to deal with these issues, two important improvements are made: (1) advanced algorithms allowing detection of events that occur over length shorter than one-half of the spatial resolution and (2) appropriate sensor design and installation procedures, allowing for controlled strain redistribution over a length compatible with algorithm requirements and sensor mechanical properties, have been developed. These improvements were tested in laboratory and on-site, and presented in Ref. 15. They are briefly summarized in this article.

The distributed temperature and strain monitoring system is based on the change in Brillouin frequency of the scattered light in optical fiber. For every point of a distributed sensor, an average Brillouin frequency diagram is created by resolving the integral of amplitudes for different scanning frequencies over the spatial resolution. An example of an average Brillouin frequency diagram in a point of sensor, obtained with spatial resolution of 1 m, is given in Figure 5(a).

If the event that changes Brillouin frequency (strain or temperature change) occurs over a length which is shorter than the spatial resolution, but longer than half of the spatial resolution, this event will be detected and localized by main peak, but not accurately measured. However, should the event occur over the length that is shorter than half of the spatial resolution, but still longer than a tenth of the spatial resolution, then due to small integration length this event will not be detected within the main peak, but will create a secondary peak in the Brillouin frequency diagram.<sup>16</sup> An example of a secondary peak created with spatial resolution of 1 m, and localized strain of approximately  $4000 \mu\epsilon$  applied over 10 cm is given in Figure 5(b).

Crack opening is a typical event that may create localized change in Brillouin frequency, thus the diagram presented in Figure 5(b) actually corresponds to the crack opening of 0.4 mm that acts over the length of sensing fiber of 10 cm. The secondary peak is not detected directly, using the same detection scheme as for the main peak and it is not visible in the diagram of the main Brillouin trace. It is detected using a special identification algorithm implemented in software and presented in diagram in form of spots.<sup>16</sup> These spots will be referred to as ‘crack spots’ in the further text.

Several laboratory tests under controlled conditions were performed in order to evaluate the performance of the implemented algorithm. Tests consisted of tensioning 10 cm of optical fiber for different pre-defined values using the set-up presented in Figure 6(a). The tests assumption is that the crack opening does not involve only one point at the optical fiber, but it rather redistributes over 10 cm length, and creates a uniform strain along these 10 cm. The reason for this approach is explained later in this Section. Tests confirmed excellent performance in terms of detectable crack opening, which was better than 0.35 mm over 10 cm, and in terms of reliability – all the simulated crack openings were successfully detected and localized. Summary of results is given in Figure 6(b).

Provided that the sensor is continuously bonded to the structure along its length, a crack in the structure generates concentrated strain and stress in the sensor at the crack location. The stress generated by the crack is very high and there is a risk of breakage. On the other hand, the crack identification algorithm functions only if local stress is redistributed over a minimum length of 10 cm.

To solve both issues, it was decided to create a mechanism of sensor delamination at the crack location. The adhesive used is carefully selected in order to allow delamination of the sensor over a length not shorter

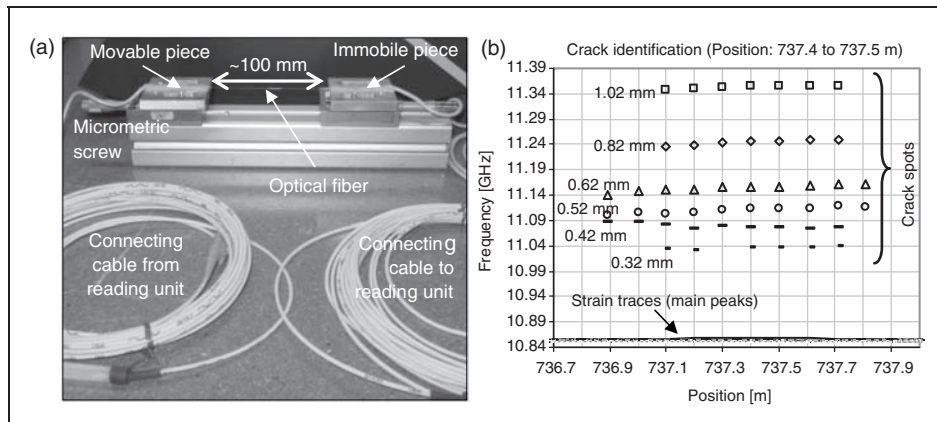


**Figure 6.** Crack algorithm testing set-up (a) and summary of results with successful crack detection (b).

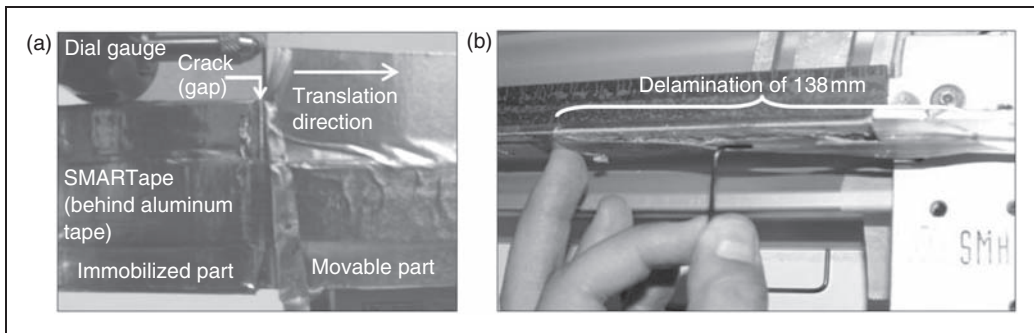


**Figure 7.** Delamination testing set-up before crack simulation (a) and during the crack simulation (b).

than 10 cm in the case of a crack opening of 0.5 mm or more. Delamination will help avoid breakage of sensor by redistribution of the strain over a minimum 10 cm; in the case of a crack opening of 0.5 mm this amounts to 0.5%, which is within the strength limits of both components of sensor, composite tape and optical fiber. Delamination also provides necessary strain redistribution for correct functioning of the crack identification algorithm.

The delamination mechanism, selected adhesive and installation procedures were tested in the laboratory in order to evaluate their performance. A special set-up was built. The sensor was glued to metallic supports that were then exposed to relative translation movement simulating crack opening. The relative translation movement was ensured by special metallic holders that forced the metallic supports to slide over straight lines and prevented all types of rotations. One metallic support was immobilized while the other was movable. Translation was imposed by a micrometric screw and the relative displacement between two metallic supports was controlled using a dial gauge. The set-up is presented in Figure 7(a).

The gap, simulating a crack, was opened to 0.5 mm. Delamination was noticed by characteristic noise, and

verified visually. The initial delamination length was between 130 and 140 mm, i.e. bigger than tenth of spatial resolution of the system. After initial delamination was formed, due to strong forces in the testing set-up, the gap opening slowly increased by 30%, while the length of delamination increased slowly in time by 50% approximately and stabilized after a few days, when the shear stresses at adhesive interfaces drops below the adhesion resistance. The increase of delamination length causes a decrease of the force in the sensor and consequently a decrease in the shear stresses at adhesive interfaces, leading to eventual stabilization of delamination after a few days. Further increase in the crack opening may cause increase in delamination length, however this does not decrease performance of the monitoring system. Should the length of delamination exceed the half of the spatial resolution, the crack will be detected not by 'crack spots', but by main trace (see Figure 4, and also large scale test presented later in the text).

The results of delamination tests proved the delamination mechanism and confirmed good selection of adhesive and installation procedures. The results of the delamination test reflect the adhesive behavior in laboratory conditions and in short-term. The selected

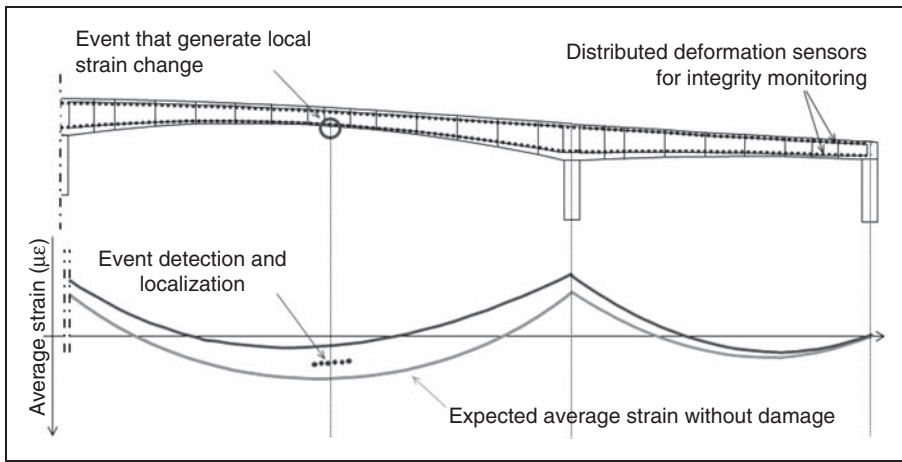


**Figure 8.** Schematic representation of integrity monitoring (schematic representation only, does not refer to a real case).

adhesive was proven over several years in the other on-site applications carried out by authors.<sup>14</sup> Although it is impossible to predict the long-term behavior of adhesive for every bridge site, based on tests and previous experiences it is reasonable to assume its good performance. An example of a delaminated sensor after removal of protective aluminum tape is given in Figure 7(b).

It is important to highlight that the redistribution of the 0.5 mm crack opening over the delaminated length of the sensor creates a localized strain change in the sensor of several thousands of microstrains, depending on the true length of delamination (see the difference in magnitude between the main trace and the crack spots in Figure 6, gauge factor is approximately  $5 \cdot 10^{-5}$  GHz/microstrain or .001 GHz  $\sim$  20 microstrains). This high localized strain change provides with high reliability in crack detection, since it cannot be overwhelmed ('masked') by the strain changes induced by usual live loads and environmental influences (e.g. thermally induced strain). In a non-impaired structure, the usual live loads and environmental influences generate significantly lower strains, and the strain distributions do not feature localized strain concentrations. The strain changes due to live loads and environmental influences that reach the range of thousands of microstrains or feature localized concentrations are per se the indicators of unusual structural behaviors (e.g. damage or overloading).

After a series of successful laboratory tests that confirmed the capability of the system to detect and localize crack occurrence with opening not smaller than 0.5 mm, the system is installed on the bridge and full-scale crack tests were performed.<sup>15</sup> The results of tests confirmed good performance of the implemented crack detection method. Detailed description and analysis of the full-scale tests is presented in a separate journal paper.<sup>17</sup>

In summary, damage that occurs in the form of local strain changes can be detected using a distributed sensor either as a change in strain measurement (change in main trace), if it affects a sensor segment that is longer than half of the spatial resolution of the system (see Figure 4(b)), or by 'crack spots' if the damage affects a sensor segment with length between one-tenth and one-half of the spatial resolution (see Figure 4(c)).

## Integrity monitoring

By term 'integrity' we refer to the quality of being whole and complete, or the state of being unimpaired. A distributed deformation sensor can be installed over the whole length of the monitored structural member, and therefore provide for direct detection and localization of local strain changes generated by damage. Thus, it provides for the integrity monitoring of the instrumented locations over entire length of the structure. The principle of integrity monitoring is schematically presented in Figure 8.<sup>14</sup>

In Figure 8, two distributed sensors are installed along the length of a bridge, one sensor at the top of the cross-section and the other at the bottom (dashed lines). Let us assume that the expected strain distribution due to some usual load (e.g. dead load) at the time of installation of sensors is as shown in the figure. This strain distribution cannot be measured by sensors (since generated before the sensor installations). Let us assume that an event (e.g. crack) causes a strain concentration in the sensor installed at the bottom of the cross-section as shown by small circle in the figure. If the damage is small to cause the change in static system of the structure, then it will be identified by crack spots (as shown in the figure) or by very localized strain change detected by the main trace (as shown in Figure 4(b)). However, if the damage is big enough to

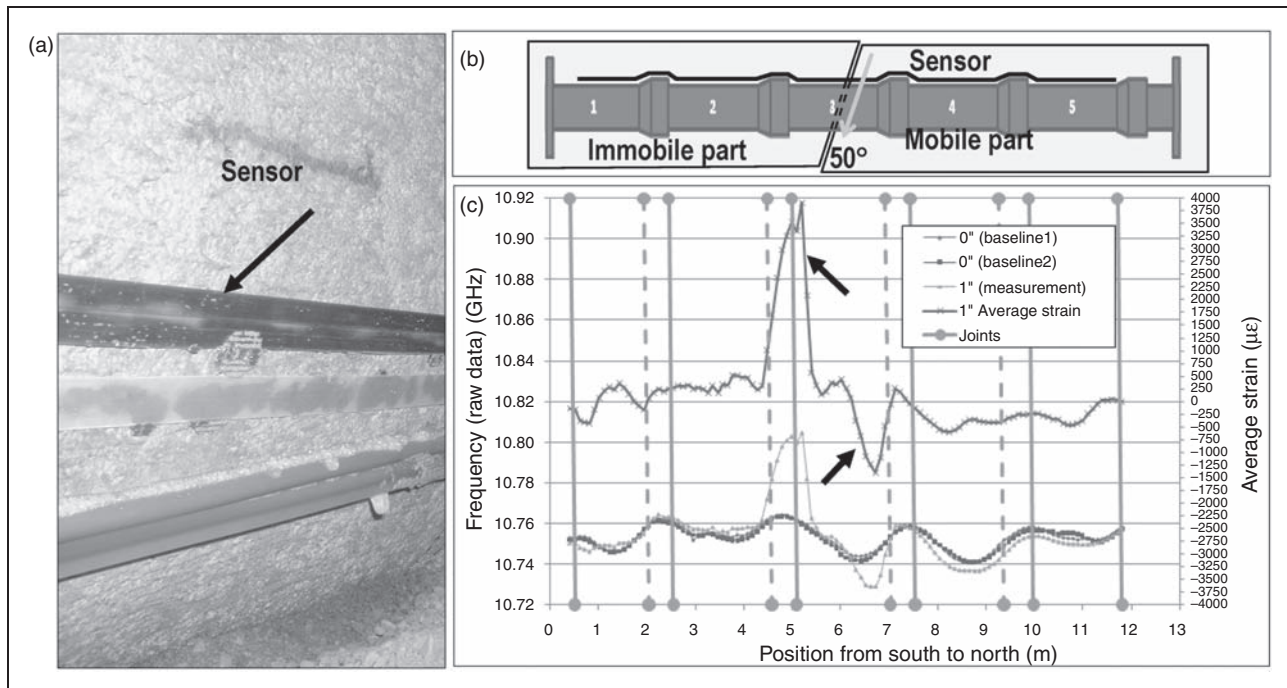


**Figure 9.** (a) Distributed sensor bonded to pipe, (b) plane view of test bed, and (c) results of test with detected damage (indicated by arrows).

cause the change in the static system of the structure, then the strain distribution along the bridge will change (e.g. as shown by dark gray line in the figure) and difference between two strain distributions will be measured by the sensors in addition to event (crack) detection.

Thus, besides the integrity monitoring, the distributed sensors can be used for curvature and deformed shape monitoring. Two parallel distributed sensors installed parallel to the elastic line of the girder provide for curvature monitoring,<sup>14</sup> and deformed shape can be then determined by double integration of curvature. Typical bridge structural members that are candidates for integrity monitoring are long beams, girders, decks, and suspension cables. Integrity monitoring can be also applied to other large structures such as dams, dikes, tunnels, and pipelines.

### Large-scale test on concrete pipe

A large scale test was performed on a pipeline with the aim to develop a method for implementation of a distributed fiber-optic system and to provide a reliable means for real-time, automatic or on-demand, assessment of pipelines subject to earthquake-induced permanent ground displacement. Besides the primary aim, the test helped evaluate the performance of distributed sensors in close-to-real conditions and their ability to detect damage. A detailed description of the test

exceeds the scope of this article and can be found in literature;<sup>18</sup> only results relevant to the contents of the article are presented.

An approximately 13-m long concrete pipe with outer diameter of 30.48 cm (12 inch) consisting of five segments was buried in the soil and exposed to shear ground movement. The distributed sensor was bonded along the pipe. Its position in the cross-section was at  $-90^\circ$  ( $0^\circ$  is top of the cross-section). A photograph of sensors installed onto the pipe is given in Figure 9(a) and a plan view of the pipe with sensors is shown in Figure 9(b).

The installation of sensor was challenging for several reasons: (i) the sensors had to be handled without twisting in order to avoid the damage of the sensor; such a handling was not easy taking into account large length of the sensor; (ii) both the surface of the structure and the sensor had to be cleaned before gluing in order to provide for good bonding of the sensor to the structure; this happened to be time consuming especially in dusty environment of the pipe; (iii) sharp edges at the pipe joints (see schematic drawing in Figure 9(b)) had to be bridged with plastic supports in order to avoid concentrated optical losses in the sensors; (iv) small bending radii of the sensor had to be avoided in order to ensure satisfactory strength of the optical signal and the durability of the installation.

All these issues were not a real obstacle for implementation of the system; however, the installation of



**Figure 10.** View to Götaälvbron.

the sensor is identified as a challenge that is to be solved by proper detailed planning depending on structure's shape and material, and the site conditions in general. Improper installation may cause damage to sensors and significantly decrease their performance. Similar experience was gathered from the on-site application on the bridge presented in the next section.

The test bed consisted of two parts, immobile and mobile. Relative translation with angle of approximately  $50^\circ$  between two parts was generated by means of hydraulic jacks. This relative ground movement of 25.4 mm (1 inch) damaged the pipe at the joints No. 2 and No. 3. The test bed is schematically presented in Figure 9(b). Measurements were performed before and after the relative ground movement was imposed. The results are presented in Figure 9(c).

Two unusual strain changes are observed, high tension close to joint No. 2 and high compression close to joint No. 3. These unusual strain changes actually correspond to locations of actual damage on the pipe. The damage was detected directly by strain measurement since the affected length of the sensor was longer than half of the spatial resolution of the monitoring system (the length of the sensors around bell-and-spigot joint was approximately 50 cm, while the spatial resolution of the system was 1 m). The results demonstrated the ability of the system to detect cracks in close-to-real conditions and in real-time. Although the test was performed on pipe, the distributed sensor would bring the same performance if applied on bridges.

### On-site application on a bridge

Götaälvbron,<sup>11,13,14</sup> the bridge over the Gota River, was built in the 1930s and is now more than 70 years old. Being one of the three communication lines that connect the two sides of the Gota River, Götaälvbron is a bridge of high importance for the city of Gothenburg (Sweden). The bridge is more than 1000 m long and consists of a concrete slab poured on nine steel

continuous girders supported on more than 50 columns. During the last maintenance work, a number of cracks were found in steel girders, notably in the zones above columns where significant negative bending moments are present. These cracks are consequences of fatigue over the many years of service and mediocre steel quality. A view of the bridge is presented in Figure 10.

The bridge is now repaired and the traffic authorities of the city of Gothenburg (Trafikkontoret) would like to keep it in service for the next 15 years, but new cracks due to fatigue can occur again. These new cracks can lead to the failure of cracked girders, which may occur suddenly since damage is generated by fatigue. That was the reason to perform continuous bridge integrity monitoring.<sup>15</sup>

The monitoring system selected for this project must provide for both crack detection and localization and for strain monitoring. Since cracks can occur at any point or in any girder, the monitoring system should cover the full length of the bridge. These criteria have led the traffic authorities to choose a truly distributed fiber-optic monitoring system based on stimulated Brillouin scattering.

Summarizing, the monitoring aim has been to perform long-term integrity monitoring of the bridge. Split into single tasks, the following specifications of the monitoring system have been requested:

1. to detect and localize new cracks that may occur due to fatigue;
2. to detect unusual short-term and long-term strain changes;
3. to detect cracks and unusual strain changes over the full length of five girders, in total 5 km;
4. to perform one measurement session every 2 h;
5. to perform self-monitoring; that is, to detect malfunctioning of the monitoring system itself;
6. to allow user-friendly and understandable data visualization;

7. to send warning messages automatically to responsible entities;
8. to function properly for 15 years.

The monitoring system was installed and successfully tested in 2007–2009. The tests included three site acceptance tests<sup>15,17</sup> followed by 1 year trial period. The traffic authorities of the city of Gothenburg, the consultant company in the project, and an independent supervisor company approved the tests and the system was officially commissioned in 2009. At the best to authors' knowledge the system is currently fully operational.

## Conclusions

Distributed sensing technologies have the unique capability of monitoring one-dimensional strain fields rather than simple strain in a large number of discrete points. Consequently, they can be installed over all the length of the structure and provide for direct damage detection, localization, and quantification. Besides the high measurement performance, they require simple connection to the reading unit, which significantly simplifies work related to cabling of the system.

A novel method for integrity monitoring of fracture critical bridges using distributed fiber optic technology based on Stimulated Brillouin scattering has been developed and presented. The integrity monitoring method is based on a crack or local deformation identification algorithm and a sensor delamination mechanism.

The method was successfully tested in laboratory and on-site, and implemented in monitoring of Götaälvbron, Gothenburg, Sweden.

## Acknowledgments

The test on pipe was supported by the National Science Foundation (NSF) under the NEES Program (grant CMMI-0936493) and performed at the NEES site at Cornell University. Kai Oberste-Ufer from Ruhr University Bochum, Germany, greatly helped installation of sensors and data analysis. The authors would like to acknowledge the personnel of the NEES site and in particular Mr. Tim Bond, manager of operations of the Harry E. Bovay Jr. Civil Infrastructure Laboratory Complex at Cornell University and Mr. Joe Chipalowski, the manager of Cornell's NEES Equipment Site, as well as the other partners in the project: Radoslaw L. Michalowski and Jerome P. Lynch, University of Michigan, Ann Arbor, MI; Russell A. Green, Virginia Tech, VA; Aaron S. Bradshaw, Merrimack College, North Andover, MA; W. Jason Weiss, Purdue University, West Lafayette, IN; and their students whose help and shared experience significantly contributed to the successful realization of the test. The presented work and Götaälvbron project could never have been realized without the precious help and participation of several persons from

several companies. The authors of this article would like particularly to thank Frank Myrvoll, Ralph Oml, Eric Lied, and Per Debloug from the Norwegian Geotechnical Institute (NGI), Norway; Benny Bergstrand, Leif Arvidson, Stefan Pup, Ingvar Larsson, and Jan Tuvert from Trafikkontoret, Sweden; Merit Enckell from the Royal Institute of Technology (KTH), Sweden; and Fabien Briffod, Fabien Ravet, Marc Niklès and André Bals from Omnisens SA, Switzerland. Great thanks to Luigi Bernasconi and Alfred Rüegsegger from 3M–Switzerland; Jens C. Kärger from Gurit, Switzerland; Milan Djurić and Igor Maletin from Minova Bemek, Sweden; Florian Thiele from the Mittweida University of Applied Sciences, Germany; and Daniele Posenato and Riccardo Belli, from SMARTEC SA, Switzerland. The authors would like to thank Mr. David Hubbell for help in improving the quality of this article.

## References

1. AASHTO LRFD Bridge Design Specifications. *American association of state highway and transportation officials*. 3rd ed. Washington, DC: American Association of State Highway and Transportation, pp. 1–1822, 2004.
2. TRB. *NCHRP synthesis 354, inspection and management of bridges with fracture-critical details, a synthesis of highway practice*. Washington, DC: Transportation and Research Board, pp. 1–75, 2005.
3. MnDOT, Bridge #9340. *I-35W over the Mississippi river at Minneapolis, MN*. Annual Bridge Inspection report, September 2001. Roseville, MN: Minnesota Department of Transportation, Metro Division, Maintenance Operations, Bridge Inspection, pp.1–33, 2002.
4. Minnesota Department of Employment and Economic Development – DEED. Economic impacts of the I-35W Bridge Collapse, 2009. [http://www.positivelyminnesota.com/Data\\_Publications/Data/Research\\_Reports/Economic\\_Development\\_Insights/Economic\\_Impacts\\_of\\_the\\_I35W\\_Bridge\\_Collapse.pdf](http://www.positivelyminnesota.com/Data_Publications/Data/Research_Reports/Economic_Development_Insights/Economic_Impacts_of_the_I35W_Bridge_Collapse.pdf), last accessed on June 20, 2011, pp. 1–1.
5. Minnesota Department of Transportation – MnDOT. I-35W St. Anthony Falls Bridge. FAQ, 2009.
6. Rytter A. *Vibration based inspection of civil engineering structures*, Ph.D. Dissertation, University of Aalborg, Denmark, 1993.
7. Posenato D, Lanata F, Inaudi D and Smith IFC. Model-free data interpretation for continuous monitoring of complex structures. *Adv Eng Informatics* 2008; 22(1): 135–144.
8. Posey R Jr, Johnson GA and Vohra ST. Strain sensing based on coherent Rayleigh scattering in an optical fibre. *Electron Lett* 2000; 36(20): 1688–1689.
9. Wait PC and Hartog AH. Spontaneous Brillouin-based distributed temperature sensor utilizing a fiber Bragg grating notch filter for the separation of the Brillouin signal. *IEEE Photonics Technol Lett* 2001; 13(5): 508–510.
10. Kurashima T, Horiguchi T and Tateda M. Distributed temperature sensing using stimulated Brillouin scattering in optical silica fibers. *Optics Lett* 1990; 15(18): 1038–1040.

11. Thevenaz L, Facchini M, Fellay A, Rober Ph, Inaudi D and Dardel B. Monitoring of large structure using distributed Brillouin fiber sensing, In: *Proceedings of 13th International Conference on Optical Fiber Sensors*, SPIE, OFS-13, 3746, Korea, Kyongju, pp.345–348.
12. Glisic B, Posenato D, Persson F, Myrvoll F, Enckell M and Inaudi D. Integrity monitoring of old steel bridge using fiber optic distributed sensors based on Brillouin scattering, SHMII-3, *The 3rd International Conference on Structural Health Monitoring of Intelligent Infrastructure*, Vancouver, Paper on conference CD. November 13-16 2007, Canada.
13. Glisic B and Inaudi D. Sensing tape for easy integration of optical fiber sensors in composite structures. In: *16th International Conference on Optical Fiber Sensors*, Nara, Japan, We 3–8, Bellingham WA: SPIE Press, 2003.
14. Glisic B and Inaudi D. *Fibre optic methods for structural health monitoring*. Chichester, UK: John Wiley & Sons, Inc, pp. 1–262, 2007.
15. Glisic B, Enckell M, Myrvoll F and Bergstrand B. Distributed sensors for damage detection and localization, In: *SHMII-4, The 4th International Conference on Structural Health Monitoring of Intelligent Infrastructure*, Paper on conference CD, July 2224, 2009, Zurich, Switzerland.
16. Ravet F, Briffod F, Glisic B, Nikles M and Inaudi D. Sub-millimeter crack detection with Brillouin based fiber optic sensors. *IEEE Sensors J* 2009; 9(11): 1391–1396.
17. Enckell M, Glisic B, Myrvoll F and Bergstrand B. ‘Evaluation of a large-scale bridge strain, temperature and crack monitoring with distributed fibre optic sensors’. *J Civil Struct Health Monit* 2011; 1: 37–46.
18. Glisic B and Oberste-Ufer K. Validation testing of fiber optic method for buried pipelines health assessment after earthquake-induced ground movement. In *Proceedings of 2011 NSF Engineering Research and Innovation Conference*, Atlanta, GA, USA, Paper on conference CD, January 47, 2011.